Directional sensing and streaming in *Dictyostelium* aggregation

Sofia Almeida
Inria, BIOCORE, Centre de Recherche Inria Sophia Antipolis — Méditerranée, 06902 Sophia Antipolis, France

Rui Dilão*
Nonlinear Dynamics Group, Instituto Superior Técnico, Av. Rovisco Pais, 1049-001 Lisbon, Portugal
(Received 11 January 2016; revised manuscript received 21 March 2016; published 5 May 2016)

We merge the Kessler-Levine simple discrete model for *Dictyostelium* cyclic adenosine monophosphate (cAMP) production and diffusion with the Dilão-Hauser directional sensing aggregation mechanism. The resulting compound model describes all the known transient patterns that emerge during *Dictyostelium* aggregation, which include the spontaneous formation of cAMP self-sustained target and spiral waves and streaming. We show that the streaming patterns depend on the speed of the amoebae, on the relaxation time for the production of cAMP, on the cAMP degradation rate, and on directional sensing. Moreover, we show that different signaling centers emerge during *Dictyostelium* aggregation.

DOI: 10.1103/PhysRevE.93.052402

I. INTRODUCTION

The social amoebae *Dictyostelium discoideum* (*Dd*) usually live as simple individual organisms in the soil leaf litter, feeding on bacteria and dividing by mitosis. Under prolongated starvation, colonies of the social amoebae *Dd* aggregate through a reaction-diffusion signaling process and later differentiate to form a pluricellular organism [1,2].

Starvation induces cells to produce cyclic adenosine monophosphate (cAMP) and also a phosphodiesterase enzyme (PDE) that degrades cAMP. cAMP is relayed to the medium and propagates as a reaction-diffusion wave, very often a spiral wave [3]. The amoebae move chemotactically in the direction of the gradient of cAMP concentration, forming a very particular pattern called streaming—a ramified network that converges into a cAMP wave signaling center, where amoebae eventually aggregate [4]. From this stage, aggregated amoebae start to climb vertically, passing by several stages of morphogenesis, and undergo cellular differentiation between two types of cells—stalk cells and spore cells—culminating in a mature pluricellular organism—the fruiting body [2].

Dictyostelium aggregation has been extensively modeled throughout the years and there are a variety of models to describe cAMP production and relaying dynamics [5–7], spiral wave breakup [8–10], amoebae movement and stream formation [11–13], among others. Despite this, the mechanisms of streaming formation remain unclear, as well as its parameter dependence.

The model developed in this work is constructed from the merging of two models—the Kessler-Levine model for cAMP production [14], and the Dilão-Hauser model of directional sensing [15]—and is thoroughly explored for several values of the parameters. The directional sensing model is used to eliminate the chemotactic wave paradox in the sense that, when the cAMP gradients are oscillatory, if the cAMP gradient slope reverses sign, amoeba cells stop moving ([2, p. 101] and [15–17]).

In the next section, we briefly describe and merge these two models. In Sec. III, we numerically explore the resulting model, and we make the bifurcation analysis of the (transient) streaming patterns that emerge during amoebae aggregation. In Sec. IV, we summarize the main conclusions of the paper.

II. MODELS AND METHODS

The model proposed by Kessler and Levine is a simple discrete model that does not incorporate the majority of biochemical features and machinery of amoeba cells, but is, nevertheless, successful in reproducing streaming patterns, without aggregation [14]. In this model, amoebae are interpreted as "bions": "simple elements that mimic the cell's behavior by a set of simple, easily computable rules" [14]. Each amoeba has an internal state that represents the availability of cAMP receptor sites, which are determined according to the following rules:

(i) State 0: the amoeba is excitable. The amoeba does not emit cAMP, but can detect local cAMP concentration c. If the cAMP local concentration is above the threshold c_T, the amoeba becomes excited, changing to state 1.

(ii) State 1: the amoeba is excited. The amoeba emits a fixed amount Δc of cAMP during τ time units. After τ, the amoeba progresses to state 2.

(iii) State 2: the amoeba is in the quiescent state. The amoeba neither emits cAMP nor can be further excited during t_R time units. After t_R the amoeba reverts to state 0. The propagation of cAMP in the medium is given by the reaction-diffusion equation

$$\frac{\partial c}{\partial t} = D\Delta c - \Gamma c + (\text{sources}), \tag{1}$$

where c is the cAMP concentration, D is the diffusion coefficient of cAMP, and Γ is the decay rate representing the degradation of cAMP due to PDE activity or natural degradation. The source term represents the local contributions of cAMP by the amoebae.

The Kessler-Levine dynamic rules are successful in reproducing the autoexcitable behavior of the system, and a propagating target wave results from the amoebae amplification

*ruidilao@tecnico.ulisboa.pt

of the signal emitted by a localized and external temporal signaling center, oscillating periodically around c_T. It also reproduces a transient streaming pattern without aggregation in the signaling center [14].

The directional sensing mechanism derived by Dilão-Hauser [15] assumes that amoebae are sensitive to the direction of propagation of the cAMP wave. This is justified by the fact that amoebae sense and follow an oscillatory gradient, but their movement is not oscillatory—chemotactic wave paradox. To overcome this paradox, it is assumed that amoebae are sensitive to the direction of propagation of cAMP, eventually driven by a diffusive process, together with the condition that if the slope of the gradient reverses sign, amoebae stop moving. We call this mechanism chemotactic directional sensing [15].

Assuming a time evolving bidimensional distribution of cAMP, described by the function $c(x,y,t)$, the direction of propagation operator ([15]) is

$$\vec{\mathcal{N}} = -\frac{1}{||\overrightarrow{\text{grad}\, c}||}\frac{\partial c}{\partial x}\text{sgn}\left(\frac{\partial c}{\partial t}\right)\vec{e}_x - \frac{1}{||\overrightarrow{\text{grad}\, c}||}\frac{\partial c}{\partial y}\text{sgn}\left(\frac{\partial c}{\partial t}\right)\vec{e}_y, \quad (2)$$

where $|\vec{\mathcal{N}}| = 1$, provided $||\overrightarrow{\text{grad}\, c}|| \neq 0$. This operator is evaluated at each spatial point with coordinates (x,y) and gives the local instantaneous direction of propagation of the cAMP. To simplify the model, we further assume that amoebae move with constant speed against the gradient of cAMP and follow the chemotactic directional sensing mechanism determined by $\vec{\mathcal{N}}$. Under these conditions, the local velocity of an amoeba is

$$\vec{v} = -v\vec{\mathcal{N}} \quad (3)$$

and v is a new speed parameter. Introducing (2) into (3), the velocity of an amoeba located at the point (x,y) is

$$\vec{v} = v\frac{1}{||\overrightarrow{\text{grad}\, c}||}\frac{\partial c}{\partial x}\vec{e}_x + v\frac{1}{||\overrightarrow{\text{grad}\, c}||}\frac{\partial c}{\partial y}\vec{e}_y, \quad (4)$$

provided

$$\text{sgn}\left(\frac{\partial c}{\partial t}\right) > 0. \quad (5)$$

If condition (5) is not verified and according to observations ([2, p. 101]), $\vec{v} = 0$. We note that if we allow amoeba motion for positive or negative values of $\frac{\partial c}{\partial t}$, asymptotically in time the motion of amoebae can diverge way from cAMP signaling centers [15].

We note that the directional sensing operator is determined by the spatial and temporal gradients of cAMP. The sensitivity of amoebae to the gradient of concentration is due to the large number of cAMP receptors (of the order of 50 000) distributed along the plasma membrane of amoebae [2]. *Dd* amoebae can detect a 1% difference in concentration of the chemoattractant between the front and the back of the cells [18,19]. The sensitivity to temporal gradients is justified by the dependence of the binding rate of cAMP to its receptors to the chemoattractant concentration, in agreement with observations [20–22].

The integration of the reaction-diffusion equation (1) is done using a method proposed by Dilão and Sainhas [23]. According to these authors, space and time scales (Δx and Δt) are not independent in diffusion and reaction-diffusion systems, and the relation between space and time scales that minimizes integration errors is

$$D\Delta t/(\Delta x)^2 = 1/6. \quad (6)$$

In the simulations presented in this paper, the amoebae are randomly distributed in a two-dimensional (2D) circle inside a 200×200 square lattice of cell side length Δx. Each amoeba is represented by their center of mass and occupies no area. The cAMP production follows the dynamics proposed by Kessler-Levine and the movement of the amoebae obeys the directional sensing condition derived by Dilão-Hauser. Equation (1) describes the propagation of the cAMP in the medium and is integrated in the circular region, with no flux boundary conditions.

III. RESULTS AND DISCUSSION

A. Propagation of cAMP with a pacemaker source; calibration

The parameters of the model have the following reference dimentionless values: $\Delta c = 15$, $c_T = 0.2$, $t_R = 20$, $\tau = 0.2$, and $\Gamma = 0.5$. These parameters were estimated to guarantee the observation of a spatial oscillatory regime of cAMP concentration. The integration time step is $\Delta t = 0.1$.

In the middle of the circular domain, we impose an oscillatory sinusoidal source of cAMP (pacemaker), with amplitude $A = 0.1$ and period $T = 300\Delta t$. The initial concentration of cAMP is set to zero in the circular domain, except at the pacemaker position. The pacemaker acts as a signaling center.

In Fig. 1 and in the video "propagation.mov" of the Supplemental Material [24], the propagation of a target wave

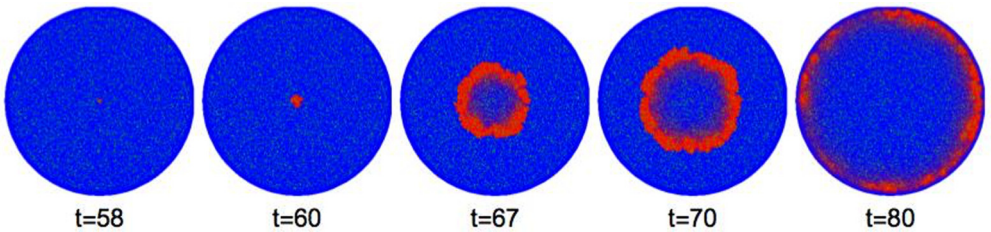

FIG. 1. Wave propagation resulting from an oscillatory cAMP signaling source imposed in the center of the circular domain. The initial concentration of cAMP is set to zero over the two-dimensional circular region. Amoebae are represented by small (green) dots. In this simulation, amoebae do not move but produce cAMP. The simulation parameters are $\Gamma = 0.5$, $t_R = 20$, $\tau = 0.2$, $\Delta c = 15$, $c_T = 0.2$, and $A = 0.1$, for a colony of 10 000 amoeba, distributed randomly in the circular region. According to the *ad hoc* estimate, time is measured in minutes. Dark gray (blue) corresponds to a low concentration of cAMP and light gray (red) to a high concentration.

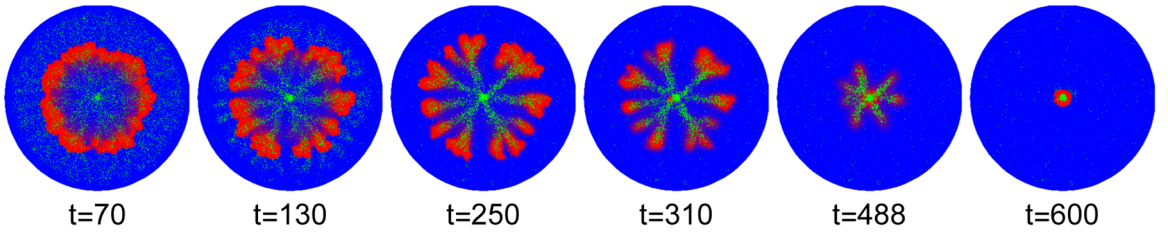

FIG. 2. Effect of directional sensing in the amoeba dynamics. We have added directional sensing to the simulations in Fig. 1. Amoebae can move with speed $v = 40$ (μm min^{-1}), following the gradient of cAMP with directional sensing. The streaming effect appears resulting in aggregation in the pacemaker region. The simulation parameters are the same as in Fig. 1, as well as the color code.

front in the 2D media is shown. In this simulation, we do not have the directional sensing effect and amoebae do not move. The purpose of this simulation is to calibrate wave speed and space-time scaling. The wave front takes about $t = 220\Delta t$ time units to propagate one radius of the circular domain, or half the size of the lattice length $100\Delta x$. Assuming that $\Delta t = 0.1$ min and as the known speed of propagation of diffusion waves in aggregating *Dd* colonies is of the order of $v = 300$ μm min$^{-1} = 5$ μm s^{-1} [14], this allows one to determine that the spatial scale of these simulations is $\Delta x = 66$ μm. By (6), we obtain for the cAMP diffusion coefficient in the medium $D = 1.21 \times 10^{-6}$ cm^2 s^{-1}, which is in the same order of magnitude of measured values, $D_{\text{measured}} = 4.4 \times 10^{-6}$ cm^2 s^{-1} [25].

Assuming this tentative calibration, the parameters of the model have dimensions $t_R = 20$ min, $\tau = 0.2$ min, and $\Gamma = 0.5$ min^{-1}; with cAMP concentrations assuming the reference units often observed in *Dd* preparations ([2, p. 102]): $\Delta c = 15$ μM, $c_T = 0.2$ μM, and $A = 0.1$ μM. In the following, we present all the simulations without specifying the units. When a parameter appears for the first time, the estimated dimensions are shown delimited by parentheses.

For these preliminary simulations, it was found that a minimum amoebae density of 27% (number of amoebae divided by the number of lattice sites inside the circle) guarantees that cAMP propagates as a reaction-diffusion wave and the parameter c_T influences the velocity of waves, with waves traveling faster for smaller values of c_T.

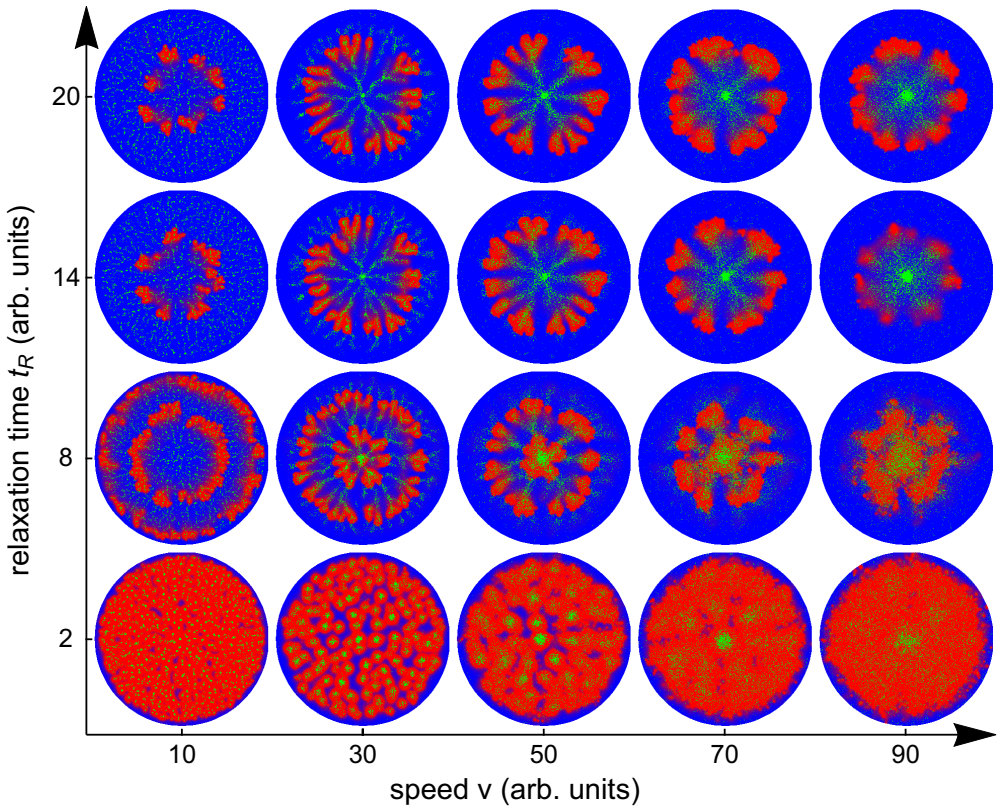

FIG. 3. Diagram for the transient states of amoebae colonies, as a function of v and t_R. These diagrams have been calculated with a colony of 10 000 amoebae with a random initial distribution, for the same parameters as in Fig. 1. The images in the figure were obtained for simulation times in the interval $t \in [240,260]$.

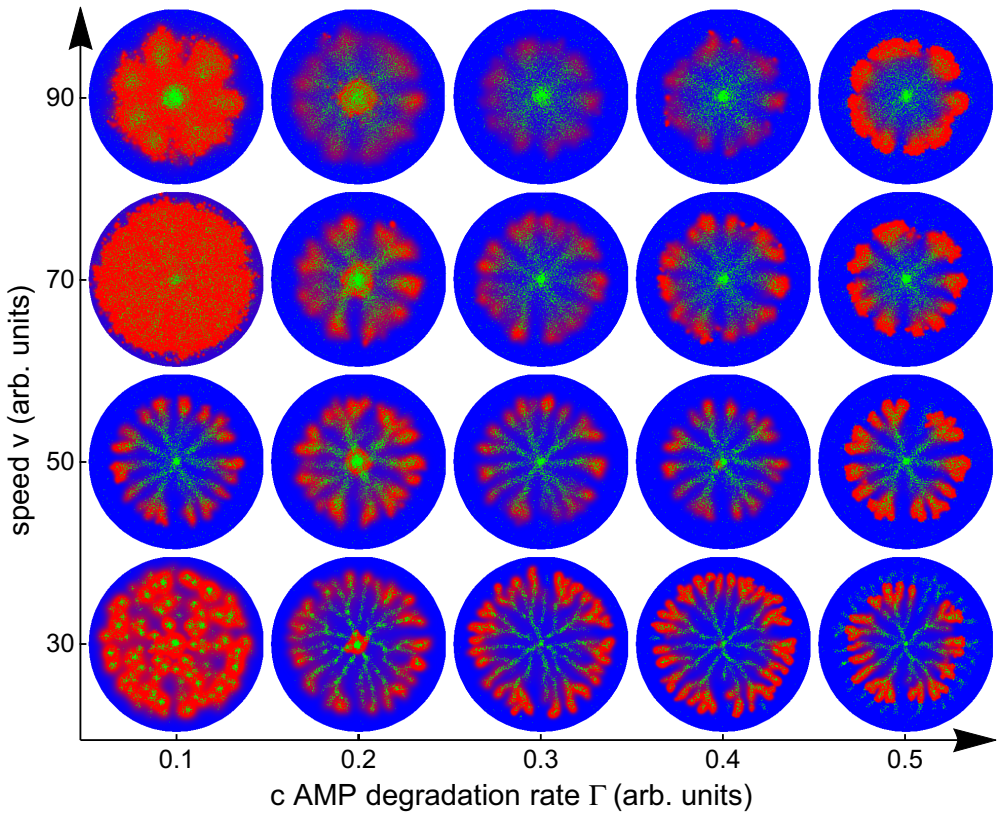

FIG. 4. Diagram for the transient states of amoebae colonies, as a function of Γ and v, for the same parameters as in Fig. 1. The images in the figure were obtained for simulation times in the interval $t \in [240,260]$.

B. Propagating cAMP and amoeba motion with directional sensing

We now set the amoebae in motion, allowing them to move only when they are on state "1," as in [14]. If condition (5) is verified locally, an amoeba in this region moves with speed v in the direction of the gradient of cAMP. In Fig. 2, we show the time evolution of 10 000 amoebae for $v = 40$ (μm min^{-1}).

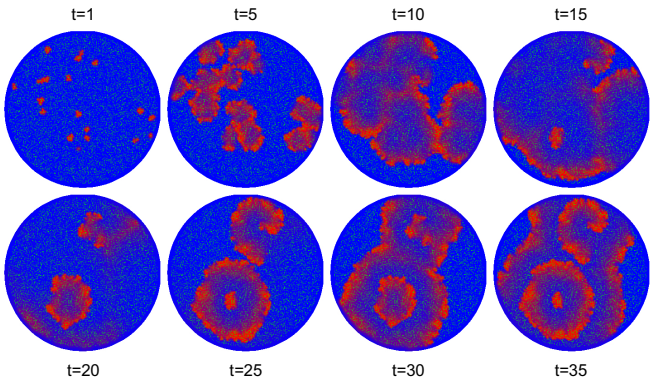

FIG. 5. Spontaneous signaling center generation over time. To the positions in space where an amoeba is located, an initial cAMP concentration $c_0 = 0.05$ per amoeba was given. As time progresses, a self-sustained rotating spiral wave and a target wave emerge. The parameters of the simulation are $\tau = 0.5, t_R = 10, \Gamma = 0.2, c_T = 0.2$, and $\Delta c = 15$.

Streaming transient patterns emerge culminating with the aggregation of all the amoebae in the signaling center, i.e., where the pacemaker is located. In the Supplemental Material [24], the video "streaming.mov" also shows this result.

The new model successfully reproduces the streaming and aggregation of *Dictyostelium* colonies. The parameters that determine the dynamics of the amoebae are the (mean) speed of the amoebae v, the degradation rate Γ, and the relaxation time t_R (which corresponds approximately to the period of cAMP emission at the pacemaker). A diagram for t_R and v, representing the transient states of the amoebae colonies, is shown in Fig. 3. To provide a general overview of the system, the diagram covers a large domain of parameters.

From the simulations in Fig. 3, we conclude that, for high oscillatory frequencies, low t_R, there is no streaming or aggregation near the cAMP source or pacemaker and the amoebae form small aggregates during time evolution. For higher t_R, there is a streaming zone, where an increase of v provokes the decreasing of the number of streams, which in turn become thicker and less defined, until streaming is no longer observed and the system enters a zone where there is aggregation without streaming. A relatively high value of t_R seems to be required to obtain aggregation in the pacemaker. Moreover, increasing the number of amoebae also interferes with the dynamics, resulting, generally, in an increase of the number of streams.

Fixing $t_R = 20$ and keeping amoebae velocity v in the streaming zone, the effects of Γ together with v are shown in the diagram in Fig. 4. In these simulations, the effects of

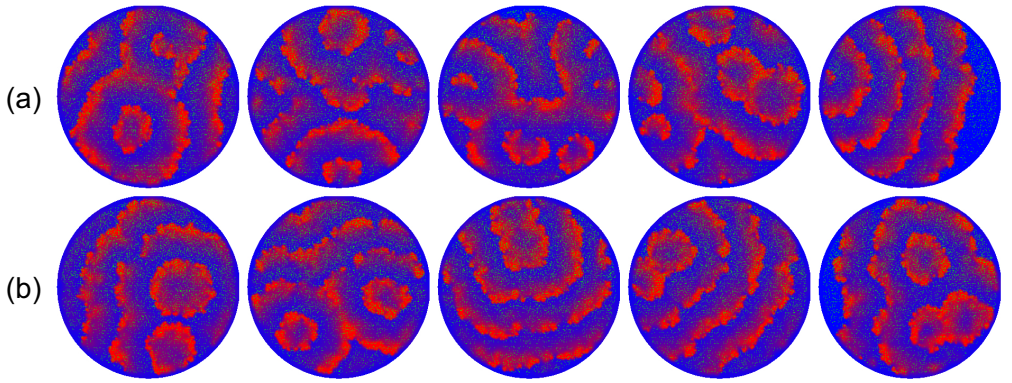

FIG. 6. Emergent waves for five different initial amoebae distributions. The number, the dynamics, and the position of the self-sustained signaling centers change: (a) $c_0 = 0.05$, (b) $c_0 = 0.08$. The other simulation parameters are $\tau = 0.4$, $t_R = 10$, $\Gamma = 0.2$, $c_T = 0.2$, and $\Delta c = 15$.

the variation of v on the system are those already discussed concerning the number and the thickness of the streams. On the other hand, lowering Γ also results in the formation of more and thinner streams, although this effect is not so pronounced. For $\Gamma \geqslant 0.6$, wave propagation does not occur anymore.

In this model, the parameters that influence the dynamics of the system are very often overlooked in experimental research. Amoebae velocity, in particular, is hardly ever addressed. The frequency of cAMP emission and the amoebae velocity together with degradation rate are at the core of the changes in the dynamics in aggregating *Dd* colonies. This simple model reproduces streaming and aggregation, allowing a straightforward understanding of the essential aspects of pattern formation.

It is important to note that the patterns obtained in Figs. 3 and 4 resemble some results obtained from experimental studies [26].

C. The emergence of spiral dynamics

It is also possible to obtain spontaneously formed spirals without an imposed pacemaker, being closer to observations [26].

With no imposed cAMP pacemaker source, to the positions in space where an amoeba is located, an initial condition of constant cAMP c_0 was given. As the amoebae only start emitting if the local concentration of cAMP is above the threshold c_T, we set $c_0 < c_T$, so that only the spatial regions with a high enough number of amoebae will have a cAMP concentration above threshold. These places act as signaling centers for a first traveling wave and, afterwards, one or more spontaneously formed signaling centers may emerge, forming self-sustained spirals or target waves. The position of second signaling centers may differ from the position of the initial ones. This process might be seen in Fig. 5, for 8 000 fixed amoebae. In the Supplemental Material [24], the video "spiral.mov" shows an animation of this simulation.

The parameters controlling the emergence and positioning of the spontaneously formed signaling centers are c_0 and the amoebae distribution. In Fig. 6, simulations are made for five different initial amoebae distributions and two different values of c_0.

Here it can be seen that the bifurcating parameters c_0 and amoebae positioning influence the emergence, the number, the position, and the dynamics of the self-sustained signaling centers. These parameters reflect directly on the initial spatial

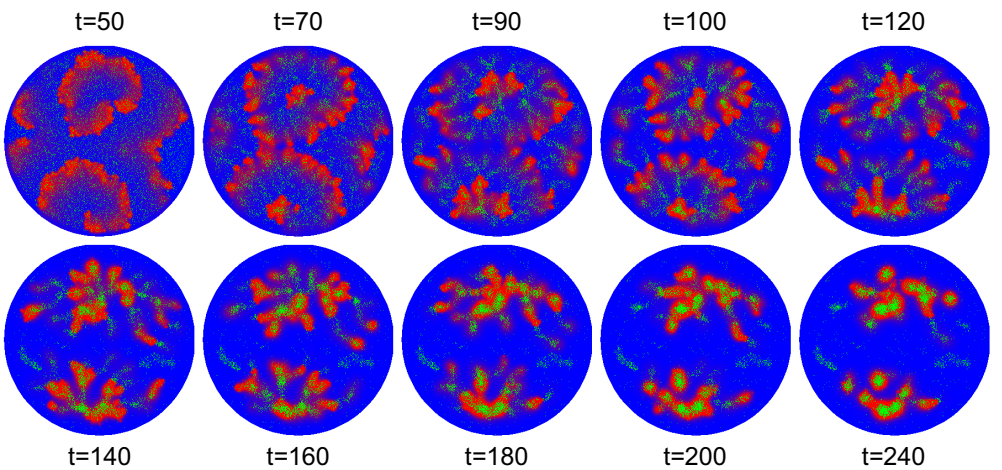

FIG. 7. Observations of streaming and aggregation together with self-sustained spiral and target wave formation. Amoebae move with speed $v = 40$. Parameters of the simulation are $c_0 = 0.2$, $\tau = 0.5$, $t_R = 10$, $\Gamma = 0.2$, $c_T = 0.2$, and $\Delta c = 15$.

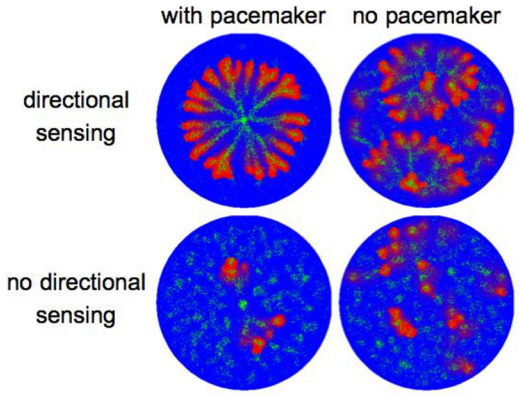

FIG. 8. Time evolution of amoebae with and without directional sensing, with pacemaker ($A = 0.1$, $c_0 = 0$) and without it ($A = 0$, $c_0 = 0.05$). The simulation parameters are $\Delta c = 15$ and $c_T = 0.2$; with pacemaker, $t_R = 20$, $\tau = 0.2$, and $\Gamma = 0.5$ at time $t = 250$; without pacemaker, $t_R = 10$, $\tau = 0.5$, and $\Gamma = 0.2$, at time $t = 100$.

distribution of cAMP, that here is seen as the essential feature behind the emergence (or not) of self-sustained signaling centers.

Introducing directional sensing in this new set of simulations, the amoebae are set in motion, and spontaneous spiral and target waves, streaming, and aggregation emerge from the dynamics. This is shown in Fig. 7, for 8500 amoebae. The video "spiralstream.mov" in the Supplemental Material [24] shows the emergence of streams, spirals. and target waves with more detail.

D. The directional sensing effect

We now analyze the effect of directional sensing in the model. In Fig. 8, we test this effect with both the imposed pacemaker and in the presence of the spontaneously established signaling centers of the previous section. It can be observed that the directional sensing effect is in fact a feature required for amoebae aggregation.

IV. CONCLUSIONS

We made a thorough analysis of a model aiming to describe the aggregation and streaming of colonies of *Dictyostelium*.

The model is successful in reproducing the essential features of *Dictyostelium* aggregation, namely, spiral and target wave formation, streaming, and emergence of signaling centers. The model is solely based on the phenomenology of the production of cAMP by excitable amoebae, cAMP diffusion, and chemotactic directional sensing.

ACKNOWLEDGMENTS

This work was supported in part by the Labex Signalife program (French National Research Agency, ANR, ANR-11-LABX-0028-01), through a fellowship to S.A. We would like to thank the anonymous reviewers of this paper for their comments.

[1] C. J. Weijer, *Dictyostelium* morphogenesis, Curr. Opin. Genet. Dev. **14**, 392 (2004)

[2] R. H. Kessin, *Dictyostelium, Evolution, Cell Biology and the Development of Multicellularity*, 1st ed. (Cambridge University Press, Cambridge, UK, 2001).

[3] S. Sawai, X.-J. Guan, A. Kuspa, and E. C. Cox, High-throughput analysis of spatio-temporal dynamics in *Dictyostelium*, Genome Biol. **8**, R144 (2007).

[4] F. Alcantara and M. Monk, Signal propagation during aggregation in the slime mould *Dictyostelium discoideum*, J. Gen. Microbiol. **85**, 321 (1974).

[5] J. L. Martiel and A. Goldbeter, A model based on receptor desensitization for cyclic AMP signaling in *Dictyostelium* cells, Biosphys. J. **52**, 807 (1987).

[6] H. Levine, I. Aranson, L. Tsimring, and T. V. Truong, Positive genetic feedback governs cAMP spiral wave formation in *Dictyostelium*, Proc. Natl. Acad. Sci. USA **93**, 6382 (1996).

[7] B. N. Vasiev, P. Hogeweg, and A. V. Panlov, Simulation of *Dictyostelium discoideum* Aggregation via Reaction-Diffusion Model, Phys. Rev. Lett. **73**, 3173 (1994).

[8] E. Palsson and E. C. Cox, Origin and evolution of circular waves and spirals in *Dictyostelium discoideum* territories, Proc. Natl. Acad. Sci. USA **93**, 1151 (1996).

[9] J. Lauzeral, J. Halloy, and A. Goldbeter, Desynchronization of cells on the developmental path triggers the formation of spiral waves of cAMP during *Dictyostelium* aggregation, Proc. Natl. Acad. Sci. USA **94**, 9153 (1997).

[10] J. J. Tyson, K. A. Alexander, V. S. Manoranjan, and J. D. Murray, Spiral waves of cyclic AMP in a model of slime mold aggregation, Physica D, **34**, 193 (1989).

[11] J. C. Dallon, B. Dalton, and C. Malan, Understanding streaming in *Dictyostelium discoideum*: Theory versus experiments, Bull. Math. Biol. **73**, 1603 (2011).

[12] J. Dallon, W. Jang, and R. H. Gomer, Mathematically modeling the effects of counting factor in *Dictyostelium discoideum*, Math. Med. Biol. **23**, 45 (2006).

[13] T. Höfer and P. K. Maini, Streaming instability of slime mold amoeba, Phys. Rev. E **56**, 2074 (1997).

[14] D. A. Kessler and H. Levine, Pattern formation in *Dictyostelium* via de dynamics of cooperative biological entities, Phys. Rev. E **48**, 4801 (1993).

[15] R. Dilão and M. J. B. Hauser, Chemotaxis with directional sensing during *Dictyostelium* aggregation, C. R. Biol. **336**, 565 (2013).

[16] K. K. Tomchik and P. Devreotes, Adenosine 3′-5′-monophosphate waves in *Dictyostelium discoideum*: A demonstration by isotope dilution-fluorography, Science **212**, 443 (1981).

[17] R. E. Goldstein, Traveling-Wave Chemotaxis, Phys. Rev. Lett. **77**, 775 (1996).

[18] S. H. Zigmond, Ability of polymorphonuclear leukocytes to orient in gradients of chemotatic factors, J. Cell Biol. **75**, 606 (1977).

[19] L. Song, S. M. Nadkarnia, H. U. Bödeker, C. Beta, A. Bae, C. Franck, W. J. Rappel, W. F. Loomis, and E. Bodenschatz,

Dictyostelium discoideum chemotaxis: Thresholds for directed motion, Eur. J. Cell Biol. **85**, 981 (2006).

[20] B. Varnum, K. B. Edwards, and D. R. Soll, *Dictyostelium* amebae alter motility differently in response to increasing versus decreasing temporal gradients of cAMP, J. Cell Biol. **101**, 1 (1985).

[21] T. Shibata, M. Nishikawa, S. Matsuoka, and M. Ueda, Intracellular encoding of spatiotemporal guidance cues in a self-organizing signaling system for chemotaxis in *Dictyostelium* cells, Biophys. J. **105**, 2199 (2013).

[22] A. Nakajima, S. Ishihara, D. Imoto, and S. Sawai, Rectified directional sensing in long-range cell migration, Nat. Commun. **5**, 5367 (2014).

[23] R. Dilão and J. Sainhas, Validation and calibration of models for reaction-diffusion systems, Int. J. Bifurcation Chaos **08**, 1163 (1998).

[24] See Supplemental Material at http://link.aps.org/supplemental/10.1103/PhysRevE.93.052402 for videos corresponding to various simulations.

[25] M. Dworkin and K. H. Keller, Solubility and diffusion coefficient of adenosine 3′:5′-monophosphate, J. Biol. Chem. **252**, 864 (1977).

[26] C. Hilgardt, Biologische Variabilität bei der Musterbildung von *Dictyostelium discoideum*, Ph.D. Thesis, Otto-von-Guericke-Universität Magdeburg, 2010.